

# **Role of protein structure in variant annotation: Review of variants causing 6-pyruvoyl-tetrahydropterin synthase deficiency and their *in-silico* functional prediction**

*Joao R.C. Muniz<sup>1#</sup>, Natalie Wing-sum Szeto<sup>2#</sup>, Rebecca Cocking<sup>1</sup>, Xian-song Wang<sup>2</sup>, Beat Thöny<sup>3</sup>, Nastassja Himmelreich<sup>4</sup>, Nenad Blau<sup>4</sup>, Kwang-Jen Hsiao<sup>5,6</sup>, Tze-Tze Liu<sup>7</sup>, Opher Gileadi<sup>1</sup>, Udo Oppermann<sup>1,8</sup>, Wyatt W. Yue<sup>1\*</sup>, and Nelson Leung-sang Tang<sup>2\*</sup>*

<sup>1</sup> Structural Genomics Consortium, Nuffield Department of Medicine, University of Oxford, UK

<sup>2</sup> Department of Chemical Pathology and Li Ka Shing Institute of Health Sciences, The Chinese University of Hong Kong

<sup>3</sup> Division of Metabolism, University Children's Hospital, Zurich, Switzerland

<sup>4</sup> Dietmar-Hopp Metabolic Center, University Children's Hospital, Heidelberg, Germany

<sup>5</sup> Department of Medical Research, Taipei Veterans General Hospital, Taiwan

<sup>6</sup> Preventive Medicine Foundation, Taipei, Taiwan

<sup>7</sup> Genome Research Center, National Yang-Ming University, Taiwan

<sup>8</sup> Botnar Research Centre, Oxford Biomedical Research Unit, UK

# Both authors contributed equally.

\* Corresponding authors: Nelson L.S. Tang and Wyatt W. Yue (wyatt.yue@sgc.ox.ac.uk; +44 (0)1865 617757)

Nelson L.S. Tang

Email: [nelsontang@cuhk.edu.hk](mailto:nelsontang@cuhk.edu.hk) (ORCID ID: 0000-0002-3607-5819)

Address: Department of Chemical Pathology, Room 38061, 1/F, Lui Che Woo Clinical Sciences Building, Prince of Wales Hospital, Shatin, New Territories, Hong Kong

Telephone: 852-2632 2960

Fax: 852-2636 5090

## ABSTRACT

Genetic defects on 6-pyruvoyl-tetrahydropterin synthase (PTPS) is the most prevalent cause of hyperphenylalaninemia **not due to phenylalanine hydrolyase deficiency (phenylketonuria)**. PTPS catalyses the second step of tetrahydrobiopterin (BH<sub>4</sub>) cofactor biosynthesis, and its deficiency represents the most common form of BH<sub>4</sub> deficiency. ~~Both untreated classical PKU and~~ PTPS deficiency result in depletion of the neurotransmitters dopamine, noradrenaline and serotonin causing neurological symptoms.

We archived reported missense variants of the *PTS* gene. Common *in-silico* algorithms were used to predict the effects of such variants and substantial proportions (up to 19%) of the variants were falsely classified as benign. We have determined the crystal structure of the human PTPS hexamer, allowing another level of interpretation to understand the potential deleterious consequences of variants from a structural perspective. The *in-silico* and structure approaches appear to be complimentary and may provide new insight that is not available from each alone. Information from the protein structure suggested that those variants affecting amino acid residues required for interaction between monomeric subunits of the PTPS hexamer were those misclassified as benign by *in-silico* algorithms. Our findings illustrated the important utility of 3D protein structure in interpretation of variants and also current limitations of *in-silico* prediction algorithms.

**Database reference:** OMIM, 261640; PDB code, 3I2B.

**Abbreviations:** BH<sub>4</sub>, tetrahydrobiopterin; HPA, hyperphenylalaninemia; TCEP, Tris(2-Carboxyethyl) phosphine hydrochloride; PTPS, 6-pyruvoyl-tetrahydropterin synthase; GTP, guanosine triphosphate; *PTS*, 6-pyruvoyl-tetrahydropterin synthase gene

## 1. INTRODUCTION

Defects in the phenylalanine metabolism are important inherited metabolic diseases (IMD) causing neurological deficits and intellectual disability. Deficiency in phenylalanine hydroxylase causing classical phenylketonuria (PKU) is the most prevalent worldwide (about 1 : 10,000 live births) <sup>1</sup>. Disorders leading to tetrahydrobiopterin (BH<sub>4</sub>) deficiency are the next common etiology of hyperphenylalaninemia (HPA). BH<sub>4</sub> is an essential cofactor for nitric oxide synthase, alkylglycerol monooxygenase, and four aromatic amino acid monooxygenases, the latter being essential for the hepatic degradation of phenylalanine and synthesis of neurotransmitter precursors of catecholamine and serotonin <sup>2,3</sup>. BH<sub>4</sub> deficiency represents a heterogeneous group of rare neurological diseases due to defective biosynthesis and recycling of BH<sub>4</sub>, where patients present with deficiency of brain catecholamines and with hyperphenylalaninemia (HPA) <sup>4,5</sup>. Clinical and biochemical data of more than 1,100 patients with inherited BH<sub>4</sub> deficiencies are tabulated in the BIoDEF database (<http://www.biopku.org>) <sup>6</sup>. This condition is also particularly prevalent in some ethnic groups in Southeast Asian populations in Southern China, Taiwan, and Thailand <sup>7</sup>.

Autosomal recessive variants on *PTS* that lead to 6-pyruvoyl-tetrahydropterin synthase (PTPS) deficiency (OMIM 261640), account for majority of BH<sub>4</sub>-defects worldwide (prevalence about 1 : 500,000 live births or 1-3% of all HPAs) <sup>8</sup>. The human *PTS* gene maps to chromosome location 11q22.3–q23.3, and consists of six exons encoding a 145 amino acid protein <sup>9</sup>. The PTPS enzyme (EC 4.6.1.10) catalyses the second reaction of the three-step *de novo* synthesis of BH<sub>4</sub> from guanosine-5'-triphosphate (GTP), namely the conversion of 7,8-dihydroneopterin triphosphate to 6-pyruvoyl-tetrahydropterin <sup>3</sup>. The severe form of PTPS deficiency causes HPA and developmental delay associated with low birthweight and parkinsonian-like features <sup>6,10</sup>, while the less common mild form gives rise to HPA only with no neurological involvement <sup>11</sup>. PTPS-deficient patients require a combined treatment with BH<sub>4</sub> to control the HPA, as well as neurotransmitter precursors (such as L-dopa/Carbidopa and 5-hydroxytryptophan) to replenish their deficit in the CNS <sup>12</sup>, although the outcome can be variable <sup>13</sup>.

Over 100 variants associated with PTPS deficiency have been reported <sup>5</sup>, most of which are missense variants, while others include termination and splicing variants. While the consequence of nonsense and frame-shift variants are easy to predict, they account for less than 10% of variants.

Missense variants lead to substitution of single amino acids at a particular codon, and their consequences can range from absolutely benign (such as those SNPs prevalent in the population) to deleterious and disease-causing. With the transformation of next-generation sequencing from a research tools to become a clinical service, there is an explosion of sequence variant data in needs of high throughput prediction of pathogenicity. In the past, sequence variants can be curated manually, and their inheritance traced in the pedigree. With hundreds of missense variants produced from a typical Exome sequence data, we have to rely on pathogenicity prediction programs such as SIFT, PolyPhen and CADD score <sup>14–16</sup>. Therefore, the performance or accuracy of these commonly-used algorithms is key to making the correct curation. Previous studies showed various limitations of these programs which had both false positive and false negative predictions <sup>17, 18</sup>.

To this end, we present the crystal structure of the human homo-hexameric PTPS enzyme PTPS for the first time here, providing an unprecedented opportunity to assess the performance of commonly used variant prediction programs on an archive of patients' variants of PTPS. Although the murine PTSP structure had been solved previously and known to be a homo-hexameric Zn(II)-metallo-enzyme, the structure of the human homologue had not been available until now. With a focus on missense variants, this study aims to determine if information from an experimentally-determined protein structure could be helpful to understand the mechanism of deleterious variants.

## 2. MATERIALS AND METHODS

### 2.1 Archive of reported missense variants in patients of PTPS deficiency

Missense variants were retrieved from multiple sources, including UniProt (<http://www.uniprot.org/uniprot/Q03393>), BioMDB (<http://www.biopku.org/home/docs/PTS.pdf>), ClinVar (<https://www.ncbi.nlm.nih.gov/clinvar/?term=PTS%5Bgene%5D>). Pubmed search to identify the original publication reporting these variants were also retrieved, and patients' phenotype were also recorded.

Only missense variants were included for further analysis and comparison of the performance of conservation based prediction algorithms and HOPE curation using 3D protein structure <sup>19</sup>.

## 2.2 Structure determination of human PTPS

### *2.2.1 Expression, purification & crystallization*

A DNA fragment encoding residues 8-145 of human PTPS (GenBank 4506331) was subcloned into pNIC28-Bsa4 vector (GenBank EF198106) incorporating an N-terminal His<sub>6</sub>-tag. The plasmid was transformed into BL21(DE3)-R3-pRARE2, cultured in Terrific Broth at 37°C, and induced with 0.1 mM IPTG for overnight growth at 18°C. Cells were homogenized, centrifuged to remove cell debris, and purified by immobilized metal affinity (IMAC) and size-exclusion chromatography. Prior to crystallization, the His-tag was removed by His-tagged TEV protease and subsequently purified by IMAC. Protein was concentrated to 17.75 mg/ml and stored in 20 mM HEPES pH 7.5, 150 mM NaCl, 5% glycerol. Crystals were grown by vapour diffusion at 4°C in sitting drops mixing 75 nl protein and 75 nl reservoir solution containing 20% PEG 3350 and 0.2 M magnesium formate. Crystals were cryo-protected in mother liquor containing 25% (w/v) ethylene glycol and flash-cooled in liquid nitrogen.

### *2.2.2 Data collection & structure determination:*

Diffraction data to 2.30 Å resolution were collected on beamline X10SA at the Swiss Light Source, and processed using the CCP4 Program suite<sup>20</sup>. The structure of hPTPS was solved by molecular replacement with PHASER<sup>21</sup>, using the rat liver PTPS structure as search model (PDB code 1GTQ, ~80% sequence identity)<sup>22</sup>. Initial automated model building was performed with ARP/wARP<sup>23</sup>, followed by cycles of iterative manual model building with COOT<sup>24</sup> and REFMAC5 refinement<sup>25</sup>. The active site metal ion was modelled as Ni(II), based on known leaching effect from nickel affinity resin in the IMAC step. The final structure factors and coordinates were deposited in the Protein Data Bank under the accession code 3I2B (Supplementary Table 1). Figures 1 and 2 showing the 3D structure models were generated using the program ICM ([www.molsoft.com](http://www.molsoft.com)).

## 2.3 Testing the accuracy of *in-silico* prediction of archived missense variants

SIFT (Sorting Intolerant from Tolerant<sup>26</sup>) and PolyPhen-2<sup>14</sup> are two commonly used online tools that are used to predict whether non-synonymous single amino acid polymorphisms may be deleterious and may affect protein function. SIFT is mainly a sequence homology based method

which estimates evolutionary conservation of residues <sup>27</sup>, and it works by blasting the query sequence against the non-redundant protein database at NCBI or UniProt <sup>28</sup> for functionally related homologous proteins. Upon sequence alignment, the program calculates the probabilities of observing the individual 20 possible amino acids in each position in the alignment, normalizes these probabilities by the most frequently naturally occurring amino acid at that position, and derives a scoring matrix from the data across species. An amino acid substitution will be classified as deleterious if the SIFT score, which is the scaled-probability of observing the particular amino acid substitution among homologous proteins, lies below a cut-off threshold, for example 0.05. The closer the score is to 0, the higher the probability the variant may be deleterious. SIFT achieved a 69% true positive rate when tested in the human diseased dataset <sup>29</sup>, while it had a 19% false positive rate <sup>26</sup> in the healthy human test dataset <sup>30</sup>.

On the other hand, PolyPhen-2 integrates results from 11 prediction algorithms, 8 of which are sequence-based and three of which are structure-based and reports a naïve Bayes probability that the substitution is damaging. This was done with the attempt to classify the concerned substitution into one of the three classes: benign (probability: 0.0-0.15), possibly damaging (0.15-1.0), or probably damaging (0.85-1.0). The closer the probability is to 1, the more likely that the variant may be damaging. PolyPhen-2 had been trained by two datasets present in UniProt, namely HumVar and HumDiv. The former is compiled from human disease-causing alleles paired with related non-damaging alleles within closely related mammalian homologues, while the latter consists of human disease alleles paired with human alleles that are not involved in disease. HumVar-trained and HumDiv-trained PolyPhen-2 achieved 73% and 92% true positive rates in an assessment of their accuracies, but with a false positive rate of 20%. The former is recommended for diagnosing Mendelian diseases with highly deleterious variants, while the latter is more sensitive and will classify even mildly deleterious variants as damaging <sup>14</sup>.

#### 2.4 Using HOPE program to curate variants against 3D protein structure

HOPE is a web based platform <sup>19</sup> that allows users to enter missense variants and it helps to map them to the 3D protein structure and provides curation on the potential effects on the known or predicted functional domains <sup>31–33</sup>. Previous evaluation by the program developing team showed promising results with the dbSNP datasets. Here we tried to see if it provided new insight to those

variants that were missed by SIFT and PolyPhen-2 (false negative variants, Table 1). Default parameters in the HOPE program was used in our analysis.

### 3. RESULTS AND DISCUSSION

#### 3.1 3D protein structure of PTPS

As part of a structural genomic effort to understand variants in human proteins involved in inborn errors of metabolism, the structure of hPTPS is determined at 2.3 Å resolution by X-ray crystallography. The hPTPS protomer (amino acids 8-144) has an elongated shape formed by a four-stranded  $\beta$ -sheet flanked by helices, bearing overall similarity with previously reported murine structure<sup>22,34</sup>. hPTPS forms a hexameric structure comprising a dimer of trimers arranged in a head-to-head manner (Fig. 1), resulting in a central 12-stranded  $\beta$ -barrel pore as seen in PTPS homologues<sup>22,34,35</sup>. Each of the six active sites in the hPTPS hexamer is located at the interface of three subunits, where it harbours (i) three conserved histidines (His24, His49 and His51) to coordinate the divalent metal ion, previously characterized as Zn(II) in the murine structure<sup>22,34</sup>; (ii) an inter-subunit triad of Cys43-Asp89-His90 that has been attributed as proton donors and acceptors during catalysis; and (iii) a Ser/Thr-Glu motif (Thr107-Glu108 in hPTPS) involved in substrate binding<sup>35</sup>.

#### 3.2 Archive of missense variant of *PTS*

To date, there are over 90 missense alleles reported to cause the severe or mild types of PTPS deficiency (Supplementary Table 2 and references therein), in addition to several splice site variants<sup>36,37</sup>. A majority of the missense variants are situated at evolutionarily conserved amino acid positions, indicating that they likely affect the function and activity of the enzyme. Among these, Asn36 and His49 are strictly invariant residues; His49 is one of the three metal coordinating histidines, while Asn36 interacts with nearby residues to maintain the structural integrity of an  $\alpha$ -helix that lines the active site pocket. Variants of either residue (Supplementary Table 2, N36K, H46R, and His49Q) resulted in the severe form of PTPS deficiency<sup>38-40</sup>.

#### 3.3 Performance of *in-silico* variant effect prediction

SIFT and PolyPhen-2 are among the variant prediction methods that are of highest speed and ease of use<sup>41</sup>. However, SIFT is incapable of processing very long sequences<sup>42</sup>. On the other hand,

although the sensitivity (true positive rate) of both SIFT and PolyPhen-2 were reported to have high sensitivity, the specificity (true negative rate) might be only around 0.5<sup>43</sup>.

As we are interested in the application of protein structure in this process, we confined to only missense variants found in PTPS patients. In keeping with previous evaluations, neither programs had a perfect sensitivity to identify deleterious variants. Among 95 variants in Supplementary Table 2, SIFT and PolyPhen-2 identified 59% (56 out of 95) and 52% (67 out of 95) (using “possibly damaging” as cut-off) of them as deleterious, respectively. With the latest reporting guideline requiring concordance of prediction programs output before variants are called deleterious, the sensitivity requiring concordance between both programs reduced to 51% (48 out of 95). Such level of sensitivity was similar to previously reported using whole genomes single nucleotide polymorphisms or Human Genetic Mutations datasets. Those variants which were wrongly predicted as benign did not cluster together or showed any recognisable features as a group.

### 3.4 Overview of variants mapped to the 3D protein structure

A mapping of the known missense variants onto the human PTPS structure shows that they are broadly distributed along the entire length of the polypeptide. It becomes apparent that many are clustered in the BH<sub>4</sub> binding region of the active site (Fig 2, purple spheres), representing a region of ‘variantal hotspot’. These variants are likely to disrupt (i) binding interactions with the BH<sub>4</sub> substrate (e.g. H49R, H49Q-) which are marked purple in Figure 2, or (ii) integrity of secondary structure elements that contribute important residues to the active site (e.g. P87S, K91E) which are marked black in Figure 2). Away from the hotspot region, further variants can be found in the central  $\beta$ -barrel pore (e.g. I18T). With the active site and the supporting structure defined, many variants could be accounted by disruption of such important structure (marked purple and black in Figure 2).

In order to see if an automatic variant interpretation algorithm based on 3D protein structure provides additional information, 20 disease-causing variants misdiagnosed (false negative) by both SIFT and PolyPhen-2 (Supplementary Table 2) were subjected to the HOPE algorithm, a web-based platform for structure-guided variant analysis. It turns out that HOPE has given a more

detailed analyses of the 20 the variants that were missed by both SIFT and PolyPhen-2. A summary of the additional information derived from HOPE is given in Table 1. As HOPE does not generate a simple score to predict if a variant is being deleterious by using the 3D structure alone, we used it to gain insight into why these 20 out of 95 (21%) of variants were falsely classified as benign by either SIFT or PolyPhen-2. Table 1 lists those variants that were false negative results of these 2 algorithms. It was found that disruption of either protein-protein contact or protein-ligand contact represented a large proportion of them. 20% of the codon position with false negative predictions were in the vicinity of metal contact, and 20% of the substituted amino acids were not of the right side-chain length to make multimer contacts. The consequence of changes in side-chain lengths, resulting in loss of ability of the mutated residues to make contacts, could only be observed by prediction software which utilized 3D protein structure analysis such as HOPE, but not SIFT and PolyPhen-2. Similarly, the prediction by HOPE showed that half of the false predictions affected the protein's secondary structure or intramolecular bonding. 30% involved charge differences which potentially disrupted salt bridge (hydrogen bond) formation. In addition, K91R<sup>7</sup> was found to be located close to the active site, thus could be damaging to the protein's function. 85% were among the observed residue types at the respective positions in homologous sequences, which could have been the cause of false negative results by conservation algorithms, as residue occurrence among homologous proteins is an important criterion for other prediction software like SIFT<sup>26</sup>. Figure 3A-F provides the distribution of the additional structural properties provided by HOPE for those misinterpreted variants by SIFT and PolyPhen-2.

### 3.5 New analysis methods are needed to interpret variant effect on protein structure

Today, when structures of most proteins are available one way or another, we propose to make use of this resource to curate SNV and visualise the effects of amino acid substitutions at any codon position. In the past, when list of variants had few entities, it was performed by manual inspection of the protein structure using PDB viewer tools. One could accommodate the side chain of the new amino acid in the existing protein and a prediction of steric hindrance was calculated. However, these predictions were not standardised and, thus, it was difficult to predict if such substitution could be accommodated<sup>44</sup>. Structure-guided pathogenicity prediction is not an easy task, also because the understanding of how protein structures bring to functions is still at its infancy.

Nowadays, it is no longer feasible as a typical WES generates a list of hundreds of missense variant, some automatic curation of the protein structure is needed. Using structure-guided prediction involving web-based tools such as HOPE is a good start, but its prediction function is still limited and need information feed from homology. Other groups have tried to make use of neural network and other algorithms to solve the classification problem <sup>31, 45, 46</sup>. However, their results still need validation in larger scale and feedback from more users.

## **ACKNOWLEDGMENTS**

Help in x-ray data collection by staff at the Swiss Light Source is gratefully acknowledged. The Structural Genomics Consortium is a registered charity (Number 1097737) funded by the Canadian Institutes for Health Research, the Canadian Foundation for Innovation, Genome Canada through the Ontario Genomic institute, GlaxoSmithKline, Karolinska Institutet, the Knut and Alice Wallenberg Innovation, Merck and Co., Inc., the Novartis Research Foundation, the Swedish Agency for Innovation Systems, the Swedish Foundation for Strategic Research and the Wellcome Trust. This work is also supported in part by the Swiss National Science Foundation grant no. 31003A-119982 (to BT). This work is part of the RD-CONNECT initiative and was supported by the FP7-HEALTH-2012-INNOVATION-1 EU Grant No. 305444 and funding from the Dietmar Hopp Foundation (both to NB). We thank David Meili and Corinne Gemperle for technical assistance on patients' variant analyses.

**Table 1: List of clinically reported variants that were false negative results on SIFT and PolyPhen-2 (misclassified as benign)**

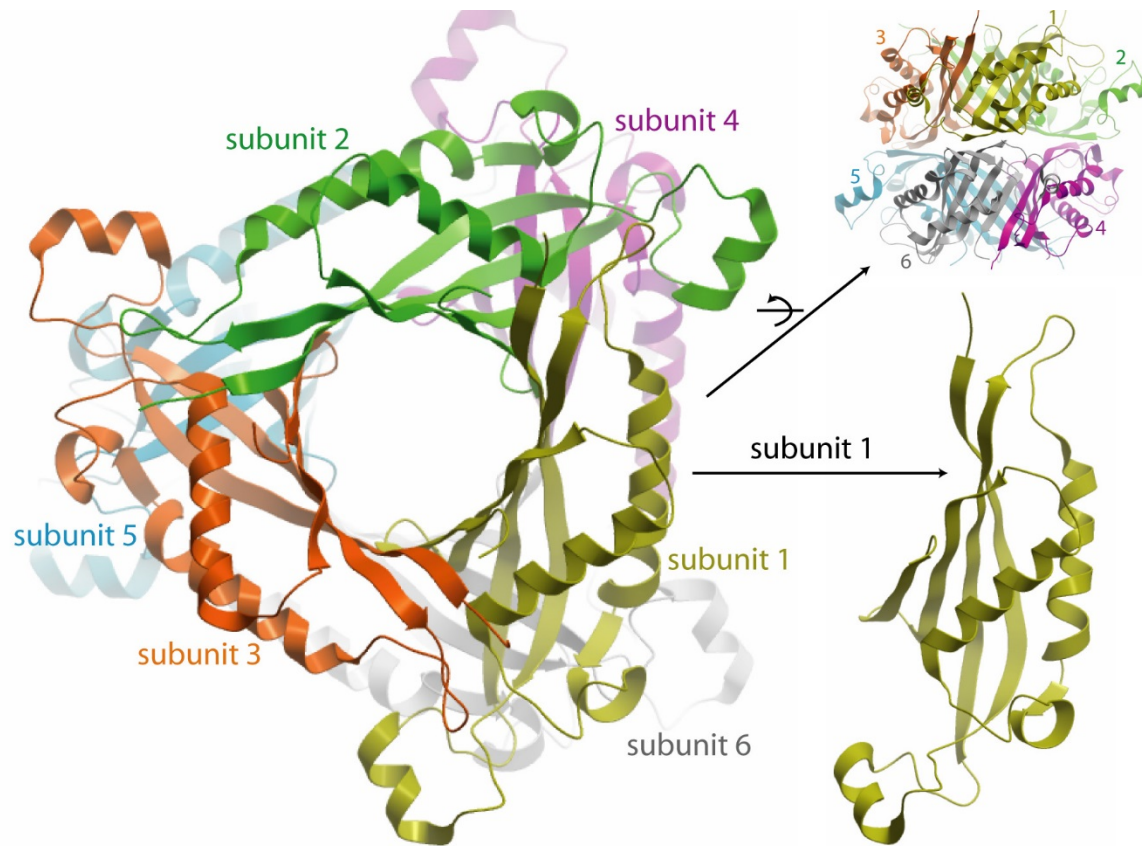
3D protein structure provides additional information about their potential effects, as shown in cyan spheres in Figure 2.

	Features of PTPS (such as 3D structure and monomer interactions) that are potentially affected by the variants, as suggested by HOPE analysis				Grouping/classification of the variant based on HOPE analysis	
	Involved in multimer contact	In the vicinity of metal contact	Forms structure	Forms salt bridge	Location of variant in protein	Variant observed in homologous proteins
R8L	Mutated residue becomes too small to form multimer contact; Change in hydrophobicity affects hydrogen bonding at multimeric contacts			Mutated residue changes from positively charged to neutral, disrupting ionic interaction at salt bridge	Surface	No
R9H	Mutated residue becomes too small to form multimer contact			Mutated residue changes from positively charged to neutral, disrupting ionic interaction at salt bridge	Surface	Yes
I18T					Core	Yes
K29T			Wild-type residue prefers alpha-helix but mutated residue doesn't		N.A.	Yes
D33G			Mutated residue (Asp) loses the flexibility that the wild-type residue (Gly) possesses for specific protein function	Mutated residue changes from negatively charged to neutral, disrupting ionic interaction at salt bridge	Surface	No, but residues with similar properties have been observed so variant may be false accepted as benign

I63V	Mutated residue becomes too small to form multimer contact				Surface	Yes
M80V			Wild-type residue prefers alpha-helix but mutated residue doesn't		Core	Yes
M80I			Wild-type residue prefers alpha-helix but mutated residue doesn't		Core, creates empty space	Yes
P87L			Mutated residue (Leu) loses the rigidity that the wild-type residue (Pro) possesses for special backbone conformation		Surface	Yes
K91R		Neighboring residue makes metal contact and may be affected by the variant		Mutated residue has no change in property but wild-type residue is involved in salt bridge formation	Close to active site	Yes
V103 A			Wild-type residue prefers beta-strand but mutated residue doesn't, destabilizing local conformation		Surface	Yes
I114V		Neighboring residue makes metal contact and may be affected by the variant			Core	Yes
N117L		Neighboring residue makes metal contact	Loss of hydrogen bonding after variant		Core	Yes

		and may be affected by the variant	in the core of the protein disturbs correct folding			
L122I					Core	Yes
V124L					Surface	Yes
G125 R			Mutated residue (Arg) loses the flexibility that the wild-type residue (Gly) possesses for specific protein function	Mutated residue changes from neutral to positively charged, disrupting ionic interaction at salt bridge	Surface	No
G125E			Mutated residue (Glu) loses the flexibility that the wild-type residue (Gly) possesses for specific protein function	Mutated residue changes from neutral to negatively charged, disrupting ionic interaction at salt bridge	Surface	Yes
K129E					Surface	Yes
D136 G	Mutated residue becomes too small to form multimer contact		Mutated residue (Gly) loses the rigidity that may be required by the protein at this position	Mutated residue changes from negatively charged to neutral, disrupting ionic interaction at salt bridge	Surface	Yes
V141F		Neighboring residue makes metal contact and may be affected by the variant			Surface	Yes

**Figure 1:** Ribbon diagram of human PTPS structure illustrating the homo-hexameric assembly. The six subunits are coloured distinctly.



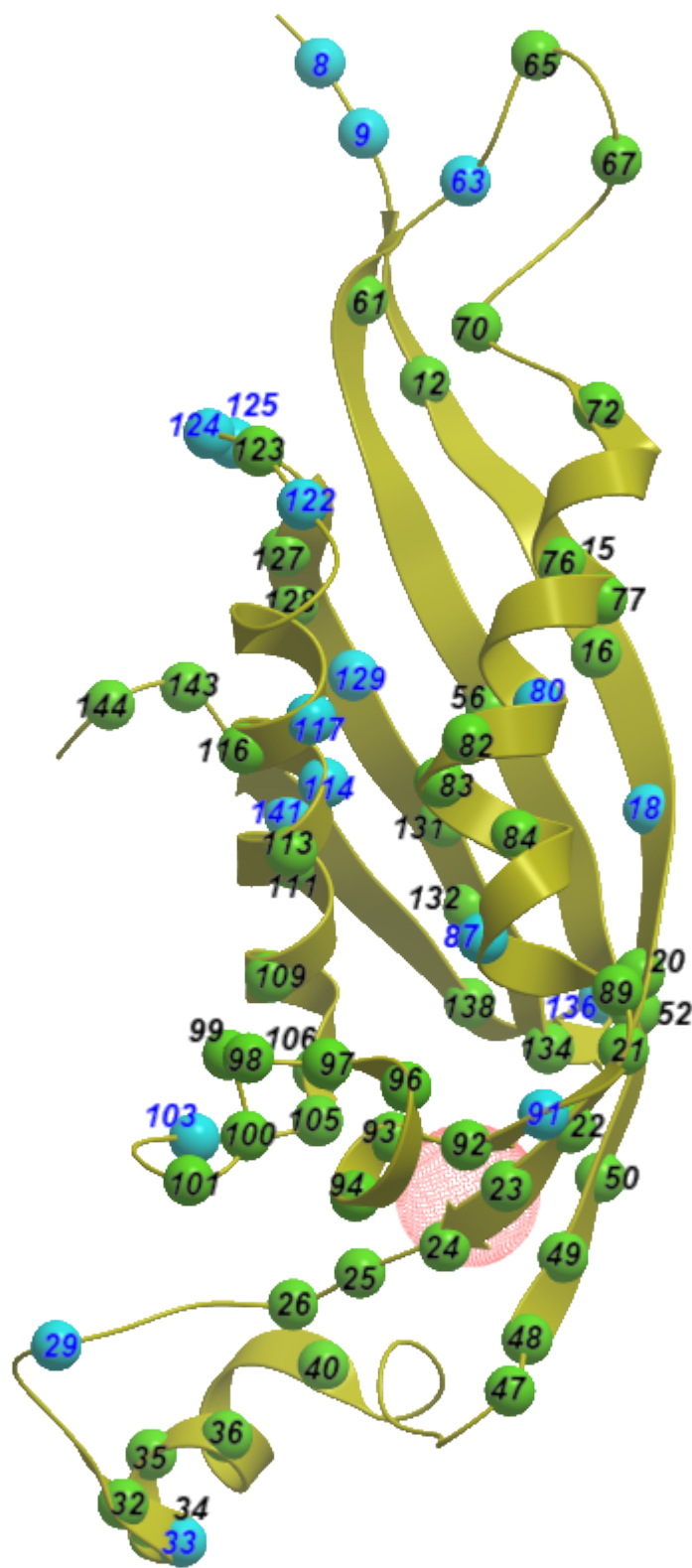
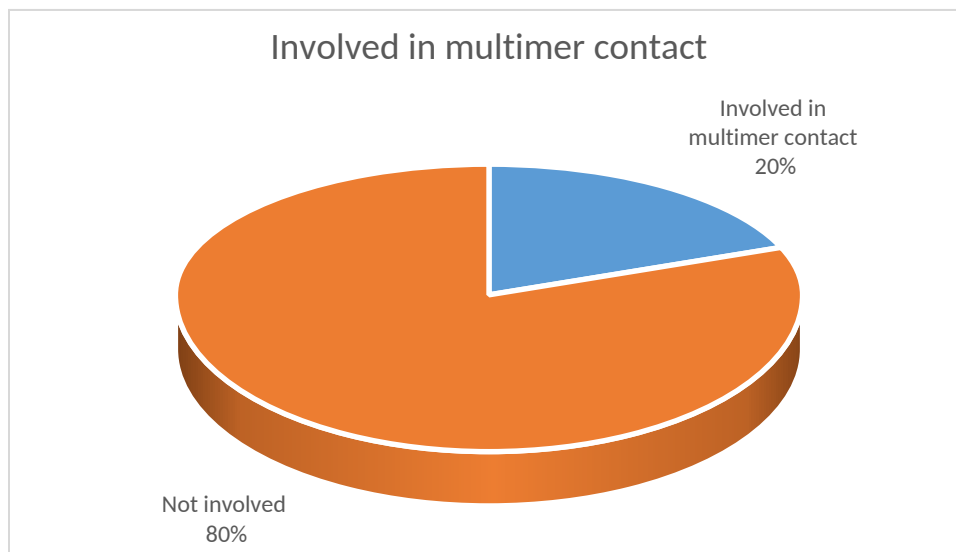


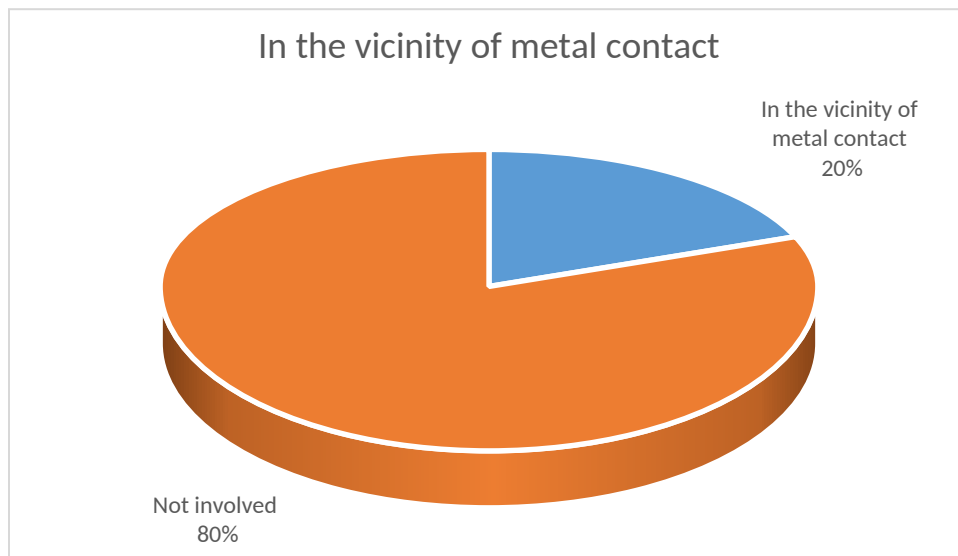
**Figure 2:** Clustering of human PTPS missense variants. The positions of amino acid variants in one PTPS protomer are indicated by spheres and numbered according to their residue number. Mutation sites described in Table 1 are shown in cyan spheres; the remainder are shown in green spheres. The active site divalent metal ion is shown in red sphere.

**Figure 3A-F:** Distribution of various functional protein features and information generated from the knowledge of 3D protein structure and curation with HOPE. 20 missense variants that were misinterpreted as benign were entered into HOPE to determine the possible effects on the protein structure and protein-ligand interaction. Proportions of these variants that (A) are involved multimeric contact, (B) are located in the vicinity of metal contact, (C) form part of the protein structure, (D) are involved in salt bridge formation, and (E) the location of the variant and (F) the frequency that the mutated residue is observed on homologous proteins, are represented as pie charts below.

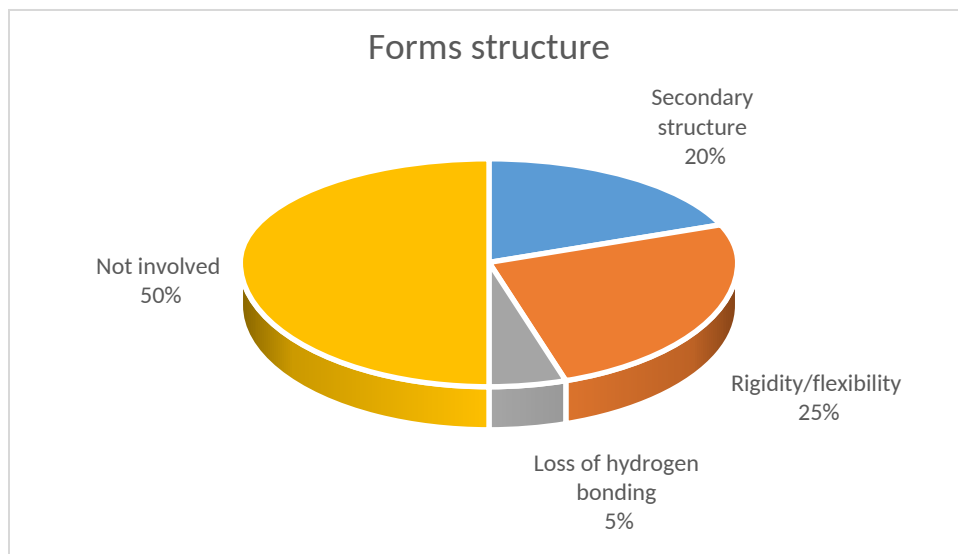
**(A)**



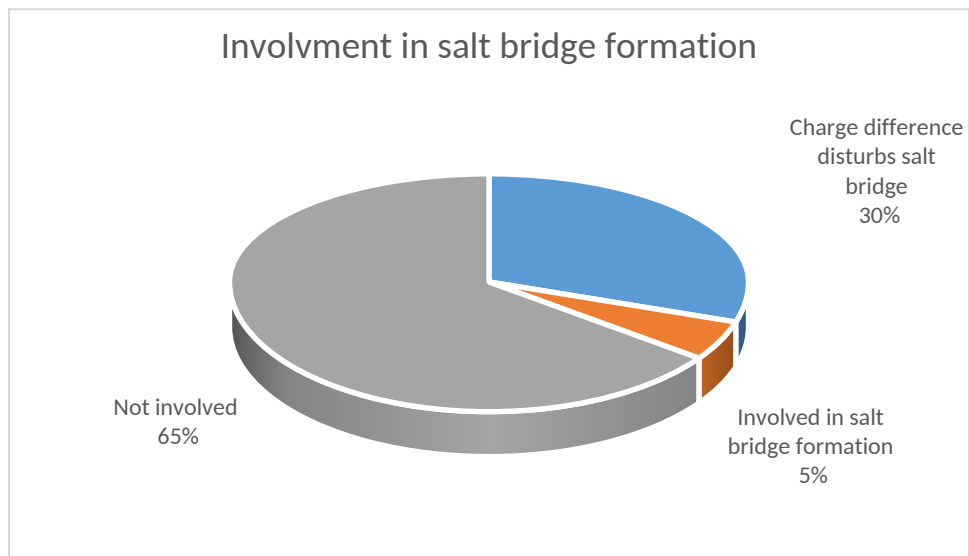
**(B)**



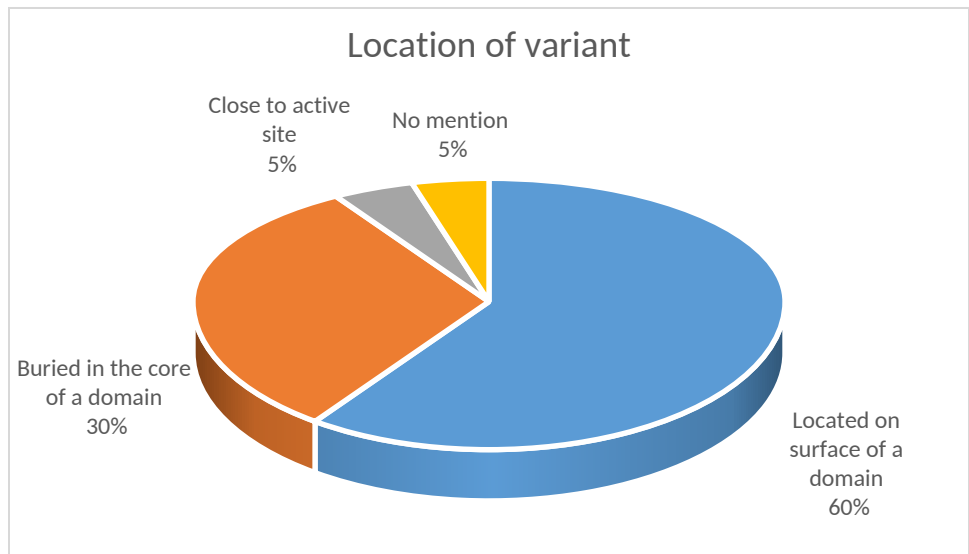
**(C)**



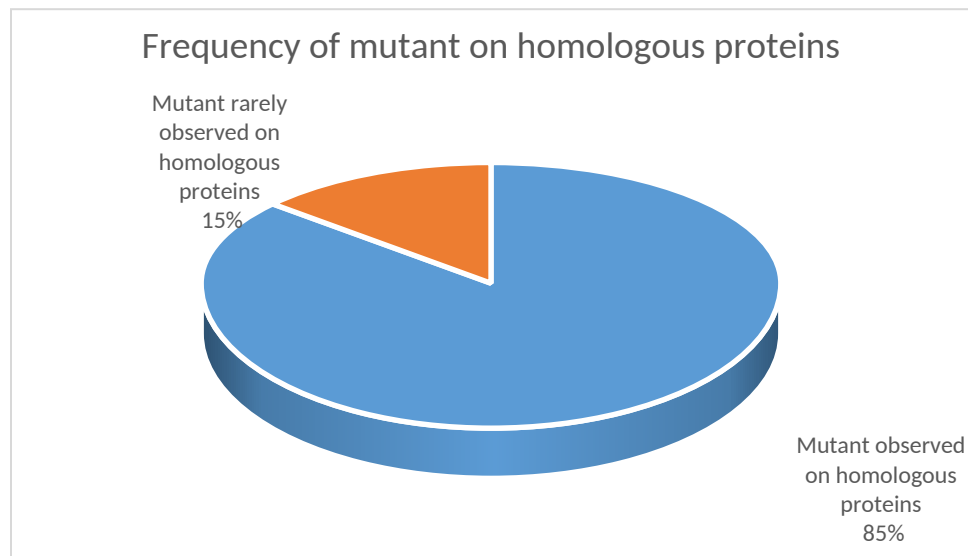
(D)



(E)



(F)



## REFERENCES

- 1 Blau N, VanSpronsen FJ, Levy HL. Phenylketonuria. *The Lancet* 2010; 376: 1417-1427
- 2 Blau N, Thöny B, Cotton RGH, *et al.* Disorders of tetrahydrobiopterin and related biogenic amines. In Scriver CR, Beaudet AL, Sly WS *et al.*, eds. *The Metabolic and Molecular Bases of Inherited Disease*. 8th ed. New York: McGraw-Hill, 2001; 1725-1776.
- 3 Werner ER, Blau N, Thöny B. Tetrahydrobiopterin: biochemistry and pathophysiology. *Biochem J* 2011; 438: 397-414
- 4 Longo N. Disorders of biopterin metabolism. *J Inherit Metab Dis* 2009; 32: 333-342
- 5 Thöny B, Blau N. Mutations in the BH4-metabolizing genes GTP cyclohydrolase I, 6-pyruvoyl-tetrahydropterin synthase, sepiapterin reductase, carbinolamine-4a-dehydratase, and dihydropteridine reductase. *Human Mutation* 2006; 27: 870-878
- 6 Opladen T, Hoffmann GF, Blau N. An international survey of patients with tetrahydrobiopterin deficiencies presenting with hyperphenylalaninaemia. *Journal of Inherited Metabolic Disease* 2012; 35: 963-973
- 7 Chiu YH, Chang YC, Chang YH, *et al.* Mutation spectrum of and founder effects affecting the PTS gene in East Asian populations. *Journal of Human Genetics* 2012; 57: 145-152
- 8 Blau N. Genetics of Phenylketonuria: Then and Now. *Human Mutation* 2016; 37: 508-515
- 9 Kluge C, Brecevic L, Heizmann CW, *et al.* Chromosomal localization, genomic structure and characterization of the human gene and a retropseudogene for 6-pyruvoyltetrahydropterin synthase. *Eur J Biochem* 1996; 240: 477-484
- 10 Jäggi L, Zurflüh MR, Schuler A, *et al.* Outcome and long-term follow-up of 36 patients with tetrahydrobiopterin deficiency. *Mol Genet Metab* 2008; 93: 295-305
- 11 Niederwieser A, Shintaku H, Leimbacher W, *et al.* 'Peripheral' tetrahydrobiopterin deficiency with hyperphenylalaninaemia due to incomplete 6-pyruvoyl tetrahydropterin synthase deficiency or heterozygosity. *Eur J Pediatr* 1987; 146: 228-232
- 12 Ogawa A, Kanazawa M, Takayanagi M, *et al.* A case of 6-pyruvoyl-tetrahydropterin synthase deficiency demonstrates a more significant correlation of L-Dopa dosage with serum prolactin levels than CSF homovanillic acid levels. *Brain Dev* 2008; 30: 82-85
- 13 Chien Y, Chiang S, Huang A, *et al.* Treatment and outcome of Taiwanese patients with 6-pyruvoyltetrahydropterin synthase gene mutations. *J Inherit Metab Dis* 2001; 24: 815-823

- 14 Adzhubei IA, Schmidt S, Peshkin L, *et al.* A method and server for predicting damaging missense mutations. *Nature Methods* 2010; 7: 248-249
- 15 Kircher M, Witten DM, Jain P, *et al.* A general framework for estimating the relative pathogenicity of human genetic variants. *Nature Genetics* 2014; 46: 310-315
- 16 Vaser R, Adusumalli S, Leng SN, *et al.* SIFT missense predictions for genomes. *Nature Protocols* 2016; 11: 1-9
- 17 Gnad F, Baucom A, Mukhyala K, *et al.* Assessment of computational methods for predicting the effects of missense mutations in human cancers. *BMC genomics* 2013; 14 Suppl 3: S7
- 18 Ghosh R, Oak N, Plon SE. Evaluation of in silico algorithms for use with ACMG/AMP clinical variant interpretation guidelines. *Genome Biology* 2017; 18: 225
- 19 Venselaar H, teBeek TA, Kuipers RK, *et al.* Protein structure analysis of mutations causing inheritable diseases. An e-Science approach with life scientist friendly interfaces. *BMC Bioinformatics* 2010; 11: 548
- 20 CCP4. CCP4 suite: programs for protein crystallography. *Acta Crystallogr D Biol Crystallogr* 1994; 50: 760-763
- 21 McCoy AJ, Grosse-Kunstleve RW, Storoni LC, *et al.* Likelihood-enhanced fast translation functions. *Acta Crystallogr D Biol Crystallogr* 2005; 61: 458-464
- 22 Nar H, Huber R, Heizmann CW, *et al.* Three-dimensional structure of 6-pyruvoyl tetrahydropterin synthase, an enzyme involved in tetrahydrobiopterin biosynthesis. *EMBO J* 1994; 13: 1255-1262
- 23 Perrakis A, Harkiolaki M, Wilson KS, *et al.* ARP/wARP and molecular replacement. *Acta Crystallogr D Biol Crystallogr* 2001; 57: 1445-1450
- 24 Emsley P, Cowtan K. Coot: model-building tools for molecular graphics. *Acta Crystallogr D Biol Crystallogr* 2004; 60: 2126-2132
- 25 Murshudov GN, Vagin AA, Dodson EJ. Refinement of macromolecular structures by the maximum-likelihood method. *Acta Crystallogr D Biol Crystallogr* 1997; 53: 240-255
- 26 Kumar P, Henikoff S, Ng PC. Predicting the effects of coding non-synonymous variants on protein function using the SIFT algorithm. *Nature Protocols* 2009; 4: 1073-1081
- 27 Hurst JM, McMillan LEM, Porter CT, *et al.* The SAAPdb web resource: a large-scale structural analysis of mutant proteins. *Human Mutation* 2009; 30: 616-624

- 28 Consortium U. Reorganizing the protein space at the Universal Protein Resource (UniProt). *Nucleic Acids Research* 2012; 40: D71-75
- 29 Ng PC, Henikoff S. Accounting for human polymorphisms predicted to affect protein function. *Genome Research* 2002; 12: 436-446
- 30 Cargill M, Altshuler D, Ireland J, *et al.* Characterization of single-nucleotide polymorphisms in coding regions of human genes. *Nature Genetics* 1999; 22: 231-238
- 31 Wiel L, Venselaar H, Veltman JA, *et al.* Aggregation of population-based genetic variation over protein domain homologues and its potential use in genetic diagnostics. *Human Mutation* 2017; 38: 1454-1463
- 32 Vihinen M. Types and effects of protein variations. *Human Genetics* 2015; 134: 405-421
- 33 David A, Sternberg MJE. The Contribution of Missense Mutations in Core and Rim Residues of Protein–Protein Interfaces to Human Disease. *Journal of Molecular Biology* 2015; 427: 2886-2898
- 34 Bürgisser DM, Thöny B, Redweik U, *et al.* 6-pyruvoyl tetrahydropterin synthase, an enzyme with a novel type of active site involving both zinc binding and an intersubunit catalytic triad motif; Site-directed mutagenesis of the proposed active center, characterization of the metal binding site and. *Journal of Molecular Biology* 1995; 253: 358-369
- 35 Ploom T, Thöny B, Yim J, *et al.* Crystallographic and kinetic investigations on the mechanism of 6-pyruvoyl tetrahydropterin synthase. *J Mol Biol* 1999; 286: 851-860
- 36 Brasil S, Vieceilli HM, Meili D, *et al.* Pseudoexon exclusion by antisense therapy in 6-pyruvoyl-tetrahydropterin synthase deficiency. *Hum Mutat* 2011; 32: 1019-1027
- 37 Meili D, Kralovicova J, Zagalak J, *et al.* Disease-causing mutations improving the branch site and polypyrimidine tract: pseudoexon activation of LINE-2 and antisense Alu lacking the poly(T)-tail. *Hum Mutat* 2009; 30: 823-831
- 38 Leuzzi V, Carducci C, Carducci C, *et al.* Phenotypic variability, neurological outcome and genetics background of 6-pyruvoyl-tetrahydropterin synthase deficiency. *Clinical Genetics* 2010; 77: 249-257
- 39 Vatanavicharn N, Kuptanon C, Liammongkolkul S, *et al.* Novel mutation affecting the pterin-binding site of PTS gene and review of PTS mutations in Thai patients with 6-

- pyruvoyltetrahydropterin synthase deficiency. *J Inherit Metab Dis* 2009; 32 Suppl 1: S279-82
- 40 Żekanowski C, Nowacka M, Sendek E, *et al.* Identification of Mutations Causing 6-Pyruvoyl- Tetrahydrobiopterin Synthase Deficiency in Polish Patients With Variant Hyperphenylalaninemia. *Mol Diagn* 1998; 3: 237-239
  - 41 Dong C, Wei P, Jian X, *et al.* Comparison and integration of deleteriousness prediction methods for nonsynonymous SNVs in whole exome sequencing studies. *Human Molecular Genetics* 2015; 24: 2125-2137
  - 42 Bendl J, Stourac J, Salanda O, *et al.* PredictSNP: robust and accurate consensus classifier for prediction of disease-related mutations. *PLoS computational biology* 2014; 10: e1003440
  - 43 Hicks S, Plon SE, Kimmel M. Statistical analysis of missense mutation classifiers. *Human Mutation* 2013; 34: 405-406
  - 44 Guex N, Peitsch MC. SWISS-MODEL and the Swiss-Pdb Viewer: An environment for comparative protein modeling. *Electrophoresis* 1997; 18: 2714-2723
  - 45 Gao M, Zhou H, Skolnick J. Insights into Disease-Associated Mutations in the Human Proteome through Protein Structural Analysis. *Structure (London, England : 1993)* 2015; 23: 1362-1369
  - 46 Mueller SC, Backes C, Kalinina OV., *et al.* BALL-SNP: combining genetic and structural information to identify candidate non-synonymous single nucleotide polymorphisms. *Genome Medicine* 2015; 7: 65

**Supplementary Table 1: X-ray data collection and refinement statistics**

<b>Data collection</b>	
Space group	P 2 <sub>1</sub> 2 <sub>1</sub> 2 <sub>1</sub>
<i>a</i> , <i>b</i> , <i>c</i> (Å)	73.3, 118.7, 34.9
$\alpha=\beta=\gamma$ (°)	90.0
Wavelength (Å)	0.9788
Resolution (Å)*	43.70 – 2.30 (2.42 – 2.30)
R <sub>merge</sub> (%)*	9.50 (79.2)
<i>I</i> / $\sigma$ <i>I</i> *	11.0 (2.1)
Completeness (%)*	100.0 (100.0)
Multiplicity*	5.0 (5.0)
<b>Refinement</b>	
No. reflections	87233
R <sub>work</sub> /R <sub>free</sub> (%)	20.8/24.6
No. atoms	
Protein	13833
Ligand/ion	12
Water	375
B-factors (Å <sup>2</sup> )	
Protein	17.03
Ligand/waters	41.50/20.12
RMS deviations	
Bond lengths (Å)	0.017
Bond angles (°)	1.483
PDB code	3I2B

\* Numbers in parentheses represent data in the highest resolution shell.

**Supplementary Table 2: Reported missense mutations in the human PTPS gene causing PTPS deficiency**

Archived missense mutations described in patients with PTPS deficiency analysed in this study and their relative predictions of variant effects by SIFT and PolyPhen-2. Position of representative codons are mapped in Figure 2, and the numerical mapping labels are shown in the rightmost column of this table. The 20 mutations that are missed by both SIFT and PolyPhen-2 are highlighted in purple.

#	Mutation site	Mutated residue	Protein change	DNA change	Exon	SIFT		PolyPhen-2		Numbering corresponding to Figure 2	Reference
						SIFT prediction	SIFT score	PolyPhen-2 prediction	Probability		
1	Met1	Val	p.M1V	c.1A>G	1	DAMAGING	0.01	benign	0.04	Not shown	1
2	Met1	Ile	p.M1I	c.3G>T/C/A	1	DAMAGING	0.02	benign	0.09	Not shown	2
3	Arg8	Leu	p.R8L	c.23G>T	1	TOLERATED	0.17	benign	0.00	8	3
4	Arg9	Cys	p.R9C	c.25C>T	1	DAMAGING	0.05	benign	0.02	9	4
5	Arg9	His	p.R9H	c.26G>A	1	TOLERATED	0.12	benign	0.02	9	5
6	Ala12	Pro	p.A12P	c.34G>C	1	DAMAGING	0.00	possibly damaging	0.60	12	1
7	Ala12	Gly	p.A12G	c.35C>G	1	DAMAGING	0.03	benign	0.03	12	3
8	Ala12	Glu	p.A12E	c.35C>A	1	DAMAGING	0.01	probably damaging	1.00	12	1
9	Ser15	Phe	p.S15F	c.44C>T	1	TOLERATED	0.55	probably damaging	1.00	15	6
10	Arg16	Cys	p.R16C	c.46C>T	1	DAMAGING	0.00	probably damaging	1.00	16	7, 8
11	Ile18	Thr	p.I18T	c.52A>C	1	TOLERATED	0.42	benign	0.20	18	4
12	Phe20	Leu	p.F20L	c.58T>C	1	DAMAGING	0.04	probably damaging	0.98	20	5
13	Ser21	Asn	p.S21N	c.62G>A	1	TOLERATED	0.28	probably damaging	1.00	21	1
14	Ser21	Arg	p.S21R	c.63C>G	1	DAMAGING	0.01	probably damaging	1.00	21	9
15	Ala22	Gly	p.A22G	c.65C>G	1	DAMAGING	0.00	probably damaging	1.00	22	10
16	Ser23	Thr	p.S23T	c.68G>C	1	DAMAGING	0.02	benign	0.00	23	5
17	His24	Pro	p.H24P	c.71A>C	1	DAMAGING	0.00	probably damaging	1.00	24	3
18	Arg25	Gly	p.R25G	c.73C>G	1	DAMAGING	0.00	probably damaging	1.00	25	11, 12
19	Arg25	Gln	p.R25Q	c.74G>A	1	DAMAGING	0.00	probably damaging	1.00	25	7, 8
20	Leu26	Phe	p.L26F	c.78G>T	1	DAMAGING	0.00	probably damaging	1.00	26	13
21	Lys29	Thr	p.K29T	c.86A>C	2	TOLERATED	0.11	benign	0.02	29	14
22	Ser32	Asn	p.S32N	c.95G>A	2	TOLERATED	0.07	possibly damaging	0.74	32	6

23	Asp33	Gly	p.D33G	c.98A>G	2	TOLERATED	0.12	benign	0.15	33	3
24	Glu34	Lys	p.E34K	c.100G>A	2	TOLERATED	0.08	possibly damaging	0.87	34	5
25	Glu35	Gly	p.E35G	c.104A>G	2	DAMAGING	0.02	probably damaging	0.98	35	10, 15
26	Asn36	Lys	p.N36K	c.108C>G	2	DAMAGING	0.00	probably damaging	1.00	36	16
27	Phe40	Leu	p.F40L	c.120T>G/A	2	DAMAGING	0.05	probably damaging	0.98	40	5, 12
28	Asn47	Asp	p.N47D	c.139A>G	2	DAMAGING	0.01	possibly damaging	0.83	47	17
29	Gly48	Asp	p.G48D	c.143G>A	2	DAMAGING	0.01	probably damaging	1.00	48	1
30	His49	Arg	p.H49R	c.146A>G	2	DAMAGING	0.00	probably damaging	1.00	49	4
31	His49	Gln	p.H49Q	c.147T>G	2	DAMAGING	0.00	probably damaging	1.00	49	18
32	Gly50	Arg	p.G50R	c.148G>A	2	DAMAGING	0.00	probably damaging	1.00	50	6
33	Asn52	Ser	p.N52S	c.155A>G	2	TOLERATED	0.25	probably damaging	1.00	52	12, 19
34	Val56	Met	p.V56M	c.166G>A	3	DAMAGING	0.04	possibly damaging	0.95	56	11, 12
35	Gly61	Arg	p.G61R	c.181G>A	3	DAMAGING	0.00	probably damaging	1.00	61	1
36	Ile63	Val	p.I63V	c.187A>G	4	TOLERATED	1.00	benign	0.00	63	14
37	Pro65	Ser	p.P65S	c.193C>T	4	TOLERATED	0.06	possibly damaging	0.46	65	1
38	Thr67	Met	p.T67M	c.200C>T	4	DAMAGING	0.00	probably damaging	1.00	67	12, 13, 16, 20
39	Thr67	Lys	p.T67K	c.200C>A	4	DAMAGING	0.00	probably damaging	1.00	67	5
40	Val70	Asp	p.V70D	c.209T>A	4	DAMAGING	0.00	probably damaging	1.00	70	11, 12
41	Asn72	Leu	p.N72L	c.216T>A	4	DAMAGING	0.00	probably damaging	1.00	72	21
42	Leu76	Phe	p.L76F	c.226C>T	4	DAMAGING	0.01	probably damaging	1.00	76	12
43	Lys77	Arg	p.K77R	c.230A>G	4	DAMAGING	0.03	possibly damaging	0.90	77	22
44	Met80	Val	p.M80V	c.238A>G	4	TOLERATED	0.68	benign	0.07	80	3
45	Met80	Thr	p.M80T	c.239T>C	4	DAMAGING	0.01	probably damaging	0.99	80	23
46	Met80	Ile	p.M80I	c.240G>T	4	TOLERATED	1.00	benign	0.00	80	3
47	Glu82	Gly	p.E82G	c.245A>G	5	DAMAGING	0.04	benign	0.02	82	3
48	Ala83	Glu	p.A83E	c.248C>A	5	TOLERATED	0.61	possibly damaging	0.86	83	6
49	Ile84	Phe	p.I84F	c.250A>T	5	DAMAGING	0.02	benign	0.27	84	22
50	Pro87	Ser	p.P87S	c.259C>T	5	TOLERATED	0.62	possibly damaging	0.90	87	12, 19, 24
51	Pro87	Leu	p.P87L	c.260C>T	5	TOLERATED	0.36	benign	0.31	87	8, 13
52	Asp89	Val	p.D89V	c.266A>T	5	DAMAGING	0.00	probably damaging	1.00	89	3

53	Lys91	Glu	p.K91E	c.271A>G	5	DAMAGING	0.03	probably damaging	0.98	91	4
54	Lys91	Arg	p.K91R	c.272A>G	5	TOLERATED	0.51	benign	0.21	91	5
55	Asn92	His	p.N92H	c.274A>C	5	TOLERATED	0.39	possibly damaging	0.71	92	25
56	Asn92	Lys	p.N92K	c.276T>A	5	TOLERATED	0.08	probably damaging	1.00	92	5
57	Leu93	Met	p.L93M	c.277C>A	5	DAMAGING	0.00	probably damaging	1.00	93	5
58	Asp94	His	p.D94H	c.280G>C	5	DAMAGING	0.00	probably damaging	1.00	94	1
59	Asp94	Gly	p.D94G	c.281A>G	5	DAMAGING	0.01	possibly damaging	0.88	94	6
60	Asp94	Val	p.D94V	c.281A>T	5	DAMAGING	0.00	probably damaging	1.00	94	26
61	Asp96	Asn	p.D96N	c.286G>A	5	DAMAGING	0.00	probably damaging	0.99	96	12, 24
62	Val97	Met	p.V97M	c.289G>A	5	DAMAGING	0.00	probably damaging	1.00	97	27
63	Pro98	Gln	p.P98Q	c.293C>A	5	DAMAGING	0.04	probably damaging	0.98	98	5
64	Pro98	Leu	p.P98L	c.293C>T	5	TOLERATED	0.07	possibly damaging	0.88	98	5
65	Tyr99	Cys	p.Y99C	c.296A>G	5	TOLERATED	0.15	probably damaging	1.00	99	28
66	Phe100	Val	p.F100V	c.298T>G	5	DAMAGING	0.01	probably damaging	1.00	100	15
67	Ala101	Val	p.A101V	c.302C>T	5	TOLERATED	0.12	possibly damaging	0.57	101	10
68	Val103	Ala	p.V103A	c.308T>C	5	TOLERATED	0.44	benign	0.01	103	4
69	Ser105	Cys	p.S105C	c.313A>T	5	DAMAGING	0.00	probably damaging	1.00	105	1
70	Thr106	Met	p.T106M	c.317C>T	6	DAMAGING	0.00	probably damaging	1.00	106	12
71	Asn109	Ser	p.N109S	c.326A>G	6	DAMAGING	0.01	probably damaging	1.00	109	25
72	Ala111	Thr	p.A111T	c.331G>A	6	TOLERATED	0.06	probably damaging	0.97	111	5
73	Ala111	Ser	p.A111S	c.331G>T	6	TOLERATED	0.08	possibly damaging	0.88	111	29
74	Tyr113	Cys	p.Y113C	c.338A>G	6	DAMAGING	0.02	possibly damaging	0.48	113	10
75	Ile114	Val	p.I114V	c.340A>G	6	TOLERATED	0.06	benign	0.23	114	30, 31
76	Asp116	Gly	p.D116G	c.347A>G	6	DAMAGING	0.05	benign	0.01	116	17
77	Asn117	Leu	p.N117L	c.351C>A	6	TOLERATED	0.40	benign	0.03	117	26
78	Leu122	Ile	p.L122I	c.364C>A	6	TOLERATED	0.34	benign	0.24	122	3
79	Pro123	Ser	p.P123S	c.367C>T	6	TOLERATED	0.10	possibly damaging	0.51	123	3
80	Val124	Leu	p.V124L	c.370G>T	6	TOLERATED	0.29	benign	0.00	124	13
81	Gly125	Arg	p.G125R	c.373G>A	6	TOLERATED	0.12	benign	0.02	125	10
82	Gly125	Glu	p.G125E	c.374G>A	5	TOLERATED	0.45	benign	0.02	125	1

83	Leu127	Phe	p.L127F	c.379C>T	6	DAMAGING	0.00	probably damaging	1.00	127	32
84	Tyr128	Asn	p.Y128N	c.382T>A	6	TOLERATED	0.11	probably damaging	0.99	128	5
85	Lys129	Glu	p.K129E	c.385A>G	6	TOLERATED	0.98	benign	0.00	129	16
86	Lys131	Asn	p.K131N	c.393A>C	6	TOLERATED	0.13	probably damaging	0.99	131	5
87	Val132	Ala	p.V132A	c.395T>C	6	DAMAGING	0.00	probably damaging	0.97	132	3
88	Glu134	Lys	p.E134K	c.400G>A	6	DAMAGING	0.00	probably damaging	1.00	134	26
89	Glu134	Asp	p.E134D	c.402A>C	6	DAMAGING	0.00	probably damaging	0.99	134	5
90	Asp136	Val	p.D136V	c.407A>T	6	TOLERATED	0.25	possibly damaging	0.82	136	13, 15, 16
91	Asp136	Gly	p.D136G	c.407A>G	6	TOLERATED	0.35	benign	0.05	136	13
92	Asn138	His	p.N138H	c.412A>C	6	DAMAGING	0.00	probably damaging	1.00	138	10
93	Val141	Phe	p.V141F	c.421G>T	6	TOLERATED	0.71	benign	0.09	141	1
94	Lys143	Asn	p.K143N	c.429A>T/C	6	DAMAGING	0.05	possibly damaging	0.83	143	6
95	Gly144	Arg	p.G144R	c.430G>C	6	DAMAGING	0.00	probably damaging	1.00	144	12

## Bibliography

- 1 Wang R, Shen N, Ye J, *et al.* Mutation spectrum of hyperphenylalaninemia candidate genes and the genotype-phenotype correlation in the Chinese population. *Clinica Chimica Acta* 2018; 481: 132-138
- 2 Stenson PD, Ball EV., Mort M, *et al.* Human Gene Mutation Database (HGMD??): 2003 Update. *Human Mutation* 2003; 21: 577-581
- 3 PNDdb. BIOPKU :: International Database of Patients and Mutations causing BH4-responsive HPA/PKU. [Accessed May24, 2018] Available from: <http://www.biopku.org/pnddb/search-results.asp>.
- 4 Leuzzi V, Carducci C, Carducci C, *et al.* Phenotypic variability, neurological outcome and genetics background of 6-pyruvoyl-tetrahydropterin synthase deficiency. *Clinical Genetics* 2010; 77: 249-257
- 5 Chiu YH, Chang YC, Chang YH, *et al.* Mutation spectrum of and founder effects affecting the PTS gene in East Asian populations. *Journal of Human Genetics* 2012; 57: 145-152
- 6 Landrum M, Lee J, Riley G, *et al.* ClinVar. In The NCBI Handbook. , 2013; 315-322.
- 7 Thony B, Leimbacher W, Blau N, *et al.* Hyperphenylalaninemia due to defects in tetrahydrobiopterin metabolism: molecular characterization of mutations in 6-pyruvoyl-tetrahydropterin synthase. *Am J Hum Genet* 1994; 54: 782-792
- 8 Oppliger T, Thöny B, Nar H, *et al.* Structural and functional consequences of mutations in 6-Pyruvoyltetrahydropterin synthase causing hyperphenylalaninemia in humans: Phosphorylation is a requirement for in vivo activity. *Journal of Biological Chemistry* 1995; 270: 29498-29506
- 9 Han B, Zou H, Han B, *et al.* Diagnosis, treatment and follow-up of patients with tetrahydrobiopterin deficiency in Shandong province, China. *Brain and Development* 2015; 37: 592-598
- 10 Friedrich-Alexander Preuß. Mutationen im PTS-Gen und mögliche Auswirkungen auf Funktion und Struktur der 6-Pyruvoyl-Tetrahydropterin-Synthase. 2001
- 11 Liu TT, Hsiao KJ, Lu SF, *et al.* Mutation analysis of the 6-pyruvoyl-tetrahydropterin synthase gene in Chinese hyperphenylalaninemia caused by tetrahydrobiopterin synthesis deficiency. *Human Mutation* 1998; 11: 76-83
- 12 Liu TT, Chiang SH, Wu SJ, *et al.* Tetrahydrobiopterin-deficient hyperphenylalaninemia in the Chinese. In *Clinica Chimica Acta*. Vol 313. , 2001; 157-169.
- 13 Dudešek A, Röschinger W, Muntau AC, *et al.* Molecular analysis and long-term follow-up of patients with different forms of 6-pyruvoyl-tetrahydropterin synthase deficiency. *European Journal of Pediatrics* 2001; 160

- 14 Trujillano D, Perez B, González J, *et al.* Accurate molecular diagnosis of phenylketonuria and tetrahydrobiopterin-deficient hyperphenylalaninemias using high-throughput targeted sequencing. *European Journal of Human Genetics* 2014; 22: 528-534
- 15 Żekanowski C, Nowacka M, Sendek E, *et al.* Identification of Mutations Causing 6-Pyruvoyl- Tetrahydrobiopterin Synthase Deficiency in Polish Patients With Variant Hyperphenylalaninemia. *Mol Diagn* 1998; 3: 237-239
- 16 Oppliger T, Thöny B, Kluge C, *et al.* Identification of mutations causing 6-Pyruvoyl-tetrahydropterin synthase deficiency in four Italian families. *Human Mutation* 1997; 10: 25-35
- 17 Scherer-Oppliger T, Matasovic A, Laufs S, *et al.* Dominant negative allele (N47D) in a compound heterozygote for a variant of 6-pyruvoyltetrahydropterin synthase deficiency causing transient hyperphenylalaninemia. *Human Mutation* 1999; 13: 286-289
- 18 Vatanavicharn N, Kuptanon C, Liammongkolkul S, *et al.* Novel mutation affecting the pterin-binding site of PTS gene and review of PTS mutations in Thai patients with 6-pyruvoyltetrahydropterin synthase deficiency. *J Inherit Metab Dis* 2009; 32 Suppl 1: S279-82
- 19 Liu TT, Hsiao KJ. Identification of a common 6-pyruvoyl-tetrahydropterin synthase mutation at codon 87 in Chinese phenylketonuria caused by tetrahydrobiopterin synthesis deficiency. *Human Genetics* 1996; 98: 313-316
- 20 Pangkanon S, Charoensiriwatanamsc W, Liamsuwanmd S. 6-pyruvoyltetrahydropterin synthase deficiency two-case report. *Journal of the Medical Association of Thailand = Chotmaihet thangphaet* 2006; 89: 872-877
- 21 Cezary Żekanowski. Diagnostyka Molekularna Wybranych Chorób Uwarunkowanych Genetycznie.
- 22 Liu N, Zhao DH, Li XL, *et al.* [PTPS gene analysis and prenatal diagnosis in patients with 6-pyruvoyl-tetra hydropterin synthase deficiency]. *Zhonghua fu chan ke za zhi* 2016; 51: 890-894
- 23 Gu MQ, Ye J, Qiu WJ, *et al.* Mutational analysis of patients with 6-pyruvoyltetrahydrobiopterin synthesis deficiency. *Chinese Journal of Medical Genetics* 2009; 26: 183-186
- 24 Imamura T, Okano Y, Shintaku H, *et al.* Molecular characterization of 6-pyruvoyl-tetrahydropterin synthase deficiency in Japanese patients. *Journal of Human Genetics* 1999; 44: 163-168
- 25 Chaiyasap P, Ittiwut C, Srichomthong C, *et al.* Massive parallel sequencing as a new diagnostic approach for phenylketonuria and tetrahydrobiopterin-deficiency in Thailand. *BMC Medical Genetics* 2017; 18
- 26 Khatami S, Dehnabeh SR, Zeinali S, *et al.* Four Years of Diagnostic Challenges with Tetrahydrobiopterin Deficiencies in Iranian Patients. In *JIMD Reports*. Vol 32. , 2016; 7-14.

- 27 Romstad A, Guldberg P, Blau N, *et al.* Single-step mutation scanning of the 6-pyruvoyltetrahydropterin synthase gene in patients with hyperphenylalaninemia. *Clinical Chemistry* 1999; 45: 2102-2108
- 28 Blau N, Scherer-Oppliger T, Baumer A, *et al.* Isolated central form of tetrahydrobiopterin deficiency associated with hemizygosity on chromosome 11q and a mutant allele of PTPS. *Human Mutation* 2000; 16: 54-60
- 29 Fernández-Lainez C, Ibarra-González I, Alcántara-Ortigoza MÁ, *et al.* Mutational spectrum of PTS gene and in silico pathological assessment of a novel variant in Mexico. *Brain and Development* 2018
- 30 Hanihara T, Inoue K, Kawanishi C, *et al.* 6-Pyruvoyl-tetrahydropterin synthase deficiency with generalized dystonia and diurnal fluctuation of symptoms: A clinical and molecular study. *Movement Disorders* 1997; 12: 408-411
- 31 Ashida A, Owada M, Hatakeyama K. A missense mutation (A to G) of 6-pyruvoyltetrahydropterin synthase in tetrahydrobiopterin-deficient form of hyperphenylalaninemia. *Genomics* 1994; 24: 408-410
- 32 Qu YJ, Song F, Jin YW, *et al.* Mutation analysis and one novel mutation detection of 6-pyruvoyl tetrahydropterin synthase gene in children with tetrahydrobiopterin deficiency. *Acta Academiae Medicinae Sinicae* 2008; 30: 170-174